Journal of Thermal Analysis, Vol. 50 (1997) 33-50

Dedicated to Prof. Menachem Steinberg on the occasion of his 65th birthday

THE THERMAL DEHYDRATION AND DECOMPOSITION OF $Ba[Cu(C_2O_4)_2(H_2O)]\cdot 5H_2O$

*J. Bacsa, D. J. Eve and M. E. Brown**

Chemistry Department, Rhodes University, Grahamstown, 6140 South Africa

Abstract

The thermal behaviour of $Ba[Cu(C_2O_4)_2(H_2O)]\cdot 5H_2O$ in N_2 and in O_2 has been examined using thermogravimetry (TG) and differential scanning calorimetry (DSC). The dehydration starts at relatively low temperatures (about 80°C), but continues until the onset of the decomposition (about 280°C). The decomposition takes place in two major stages (onsets 280 and 390°C). The mass of the intermediate after the first stage corresponded to the formation of barium oxalate and copper metal and, after the second stage, to the formation of barium carbonate and copper metal. The enthalpy for the dehydration was found to be 311±30 kJ mol^{-1} (or 52±5 kJ (mol of $H_2O)^{-1}$). The overall enthalpy change for the decomposition of $Ba[Cu(C_2O_4)_2]$ in N_2 was estimated from the combined area of the peaks of the DSC curve as −347 kJ mol^{-1}. The kinetics of the thermal dehydration and decomposition were studied using isothermal TG. The dehydration was strongly deceleratory and the α-time curves could be described by the three-dimensional diffusion (D3) model. The values of the activation energy and the pre-exponential factor for the dehydration were 125±4 kJ mol^{-1} and $(1.38\pm0.08)\times10^{15}$ min^{-1}, respectively. The decomposition was complex, consisting of at least two concurrent processes. The decomposition was analysed in terms of two overlapping deceleratory processes. One process was fast and could be described by the contracting-geometry model with n=5. The other process was slow and could also be described by the contracting-geometry model, but with n=2.

The values of E_a and A were 206±23 kJ mol^{-1} and $(2.2\pm0.5)\times10^{19}$ min^{-1}, respectively, for the fast process, and 259±37 kJ mol^{-1} and $(6.3\pm1.8)\times10^{23}$ min^{-1}, respectively, for the slow process.

Keywords: $Ba[Cu(C_2O_4)_2(H_2O)]\cdot 5H_2O$, decomposition, dehydration, kinetics

Introduction

The isothermal dehydrations and decompositions of the mixed oxalates $FeCu(C_2O_4)_2\cdot 3H_2O$, $CoCu(C_2O_4)_2\cdot 3H_2O$ and $NiCu(C_2O_4)_2\cdot 3H_2O$, have been studied recently by Coetzee and coworkers [1, 2]. The onset temperatures for

* To whom correspondence should be addressed.

0368–4466/97/ $ 5.00
© 1997 Akadémiai Kiadó, Budapest
John Wiley & Sons Limited
Chichester

the dehydration, from DSC experiments, increased in the following order: $FeCu(C_2O_4)_2 \cdot 3H_2O$ (139°C), $CoCu(C_2O_4)_2 \cdot 3H_2O$, (141°C), $NiCu(C_2O_4)_2 \cdot 3H_2O$ (202±10°C).

The thermal decompositions of these compounds were endothermic processes and took place in two overlapping stages. The mixed oxalates, $MCu(ox)_2 \cdot 3H_2O$, do not show the exothermic thermal behaviour characteristic of copper(II) oxalate. The onset temperatures for the decomposition, in N_2, from DSC experiments, increased in the order: $CoCu(C_2O_4)_2 \cdot 3H_2O$ (345°C), $FeCu(C_2O_4)_2 \cdot 3H_2O$, (351°C), $NiCu(C_2O_4)_2 \cdot 3.5H_2O$ (362°C).

The similarity of the powder diffraction patterns of $MCu(C_2O_4)_2 \cdot 3H_2O$ to those of the complexes $[M(C_2O_4)(H_2O)_2]_n$ suggested that modifying the structure of copper oxalate by introduction of other metal ions induces changes in the crystal structure so that the structure is iso-morphus with $[M(C_2O_4)(H_2O)_2]_n$. In continuation of the study of mixed metal copper oxalates, $MCu(C_2O_4)_2$, further complexes were prepared with metal ions which were chosen with large or small ionic sizes relative to the copper(II) ion (ionic radius Cu^{2+}=0.70 Å) in the hope that a change in the crystal structure would occur. An unsuccessful attempt was made to prepare the complex, $MgCu(C_2O_4)_2$ (ionic radius Mg^{2+}=0.65 Å) although the syntheses of $MgCo(C_2O_4)_2$ (ionic radius Co^{2+}=0.74 Å) and $MgNi(C_2O_4)_2$ (ionic radius Ni^{2+}=0.72 Å) were successful. An attempt to prepare anhydrous $BaCu(C_2O_4)_2$ (ionic radius Ba^{2+}=1.35 Å) was also unsuccessful, but blue crystals of the compound $Ba[Cu(C_2O_4)_2(H_2O)] \cdot 5H_2O$ were obtained. The structure of this compound has been reported [3, 4] and some thermoanalytical information has been obtained in nitrogen and in oxidizing atmosphere [3, 5].

This class of compound is of interest as possible precursors for mixed metal oxides with interesting properties such as superconductivity, and this paper reports on a detailed study of the kinetics and mechanism of both the thermal decomposition and the preceding dehydration.

Experimental

Preparation

$Ba[Cu(C_2O_4)_2(H_2O)] \cdot 5H_2O$ was prepared as follows: 100 mL of a 0.10 *M* aqueous solution of $K_2C_2O_4 \cdot H_2O$ at 35°C was stirred while 50 mL of 9.2×10^{-2} *M* $CuCl_2 \cdot 2H_2O$ solution was added dropwise from a burette. The resulting solution of $[Cu(C_2O_4)_2]^{2-}$ ions was made slightly acidic by adding 0.25 mL of glacial acetic acid. 20 mL of 1.7×10^{-1} *M* $BaCl_2 \cdot 2H_2O$ was then slowly added from a burette to the stirred solution. A pale blue, crystalline precipitate formed rapidly and was removed by filtration. The filtrate, on standing overnight, gave dark blue crystals of the product (yield=0.51 g).

Characterization

Infrared spectra were recorded using Beckman IR 4260 and Perkin-Elmer IR 180 spectrophotometers in the range 4000 to 300 cm^{-1} using the KBr disc method. Diffuse reflectance spectra were recorded using a Beckman 5240 spectrophotometer, in the range 5000 to 17000 cm^{-1}. X-ray powder diffraction patterns were obtained using a Philips diffractometer and CoK_α (1.791 Å).

Thermal analysis

Thermogravimetry (TG) and differential scanning calorimetry (DSC) were performed using Perkin-Elmer Delta Series-7 instruments. An atmosphere of N_2, at a flow rate of 15 to 20 mL min^{-1}, and sample masses of between 3 and 5 mg were used. Aluminium sample pans, covered but not crimped, were used for the DSC experiments, and open platinum sample pans were used for the TG experiments.

Stoichiometry of the thermal dehydration and decomposition

The TG curve for $Ba[Cu(C_2O_4)_2(H_2O)]\cdot 5H_2O$ heated at 10°C min^{-1} in flowing N_2 is shown in Fig. 1.

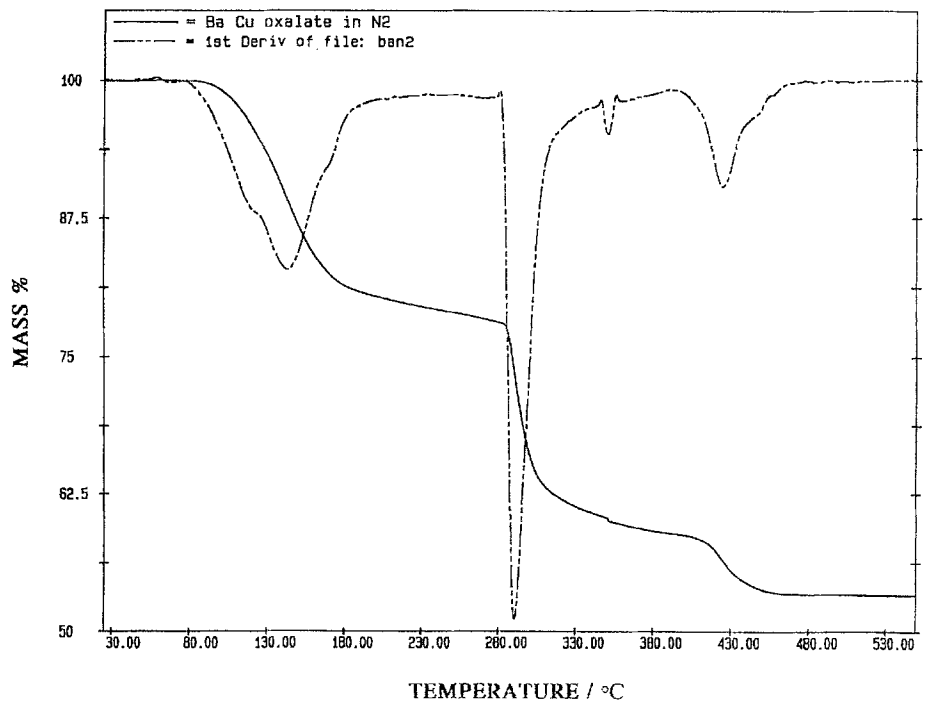

Fig. 1 TG and DTG curves for $Ba[Cu(C_2O_4)_2(H_2O)]\cdot 5H_2O$ heated at 10°C min^{-1} in flowing

Dehydration starts at 79°C and reaches a maximum rate at 144°C. The low onset temperature is due to the presence of relatively weakly held water molecules in the crystal. At 179°C, 18.6% of the sample mass has been lost, corresponding to loss of five water molecules per formula unit. At this stage the rate of dehydration has slowed down considerably and the final water is lost in a much more gradual process between 179 and 280°C. During dehydration the crystals become opaque and lighter blue as the microstructure of the crystals is destroyed. Removal of the last amounts of water coincides with the onset of the decomposition at 280°C.

Initially the decomposition is rapid, and then decelerates to a gradual mass loss. At 380°C the sample mass is 59.6% of its initial value. This mass corresponds to the formation of barium oxalate and copper metal (calculated mass=59.5%).

At 390°C a further decomposition stage occurs. A stable final mass of 53.4% of the initial mass is attained at 460°C. These results suggest that the overall decomposition (1), under these conditions, occurs in two major overlapping stages, (2) and (3):

$$Ba[Cu(C_2O_4)_2](s) \rightarrow BaCO_3(s) + Cu(s) + CO(g) + 2CO_2(g) \quad (1)$$

$$Ba[Cu(C_2O_4)_2](s) \rightarrow BaC_2O_4(s) + Cu(s) + 2CO_2(g) \quad (2)$$

$$BaC_2O_4(s) \rightarrow BaCO_3(s) + CO(g) \quad (3)$$

The final mass of the residue (53.7%) compares well with the calculated mass (53.8%) based on the formation of barium carbonate and copper metal. The formation of some CuO could not be excluded. The X-ray diffraction patterns of the residues contained no lines for either Cu or CuO. IR spectra did not show a copper(II)-oxygen band, so it was assumed that copper was present in an amorphous form. SEM showed that the final residue consists of small pseudo-crystals, typically 3 mm long. The surfaces of these particles were extensively cracked, due to the contraction of the solid and escape of product gases during the decomposition. At very high magnification, the crushed product appeared to be porous and made up of extremely small particles (typically with diameters of 0.2 μm). The final decomposition product had a sooty appearance due to the presence of carbon formed by some disproportionation of carbon monoxide.

The only infrared active material present in detectable concentrations in the final residue was ionic carbonate. The presence of barium carbonate was confirmed by XRD. The infrared spectrum of the solid intermediate isolated at 380°C showed that bridging oxalate, barium carbonate and non-bridging oxalate were present. The infrared bands of the bridging oxalate were more similar to the bands of barium oxalate than to copper oxalate. The temperature for the onset of

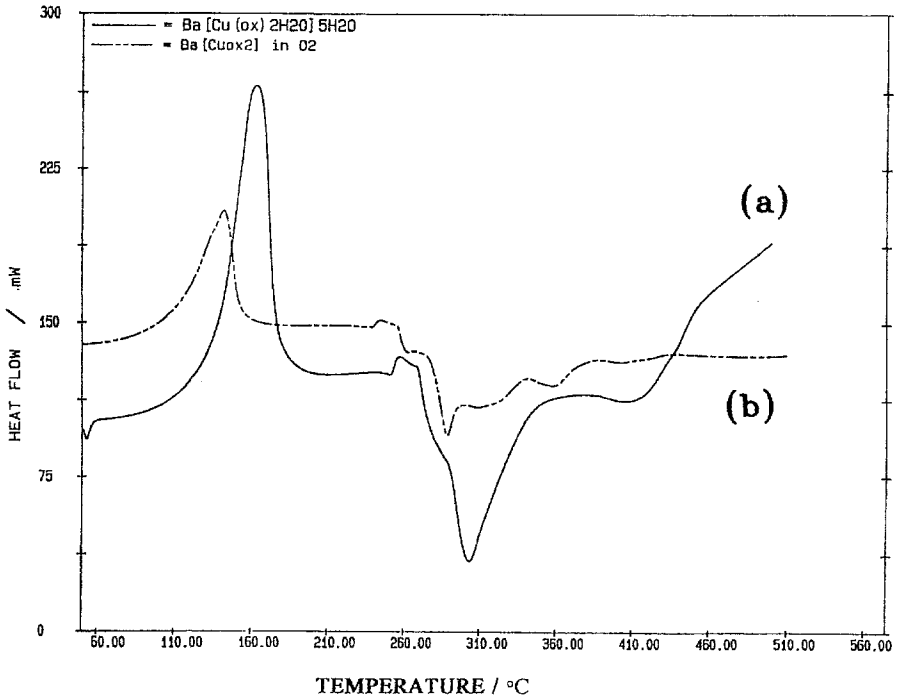

Fig. 2 DSC curves for $Ba[Cu(C_2O_4)_2(H_2O)]\cdot 5H_2O$ heated at 20°C min^{-1} (a) in flowing N_2, (b) in flowing O_2

the decomposition of barium oxalate is 400°C, compared to 270°C for copper(II) oxalate. On the basis of the mass loss data, the bridging oxalate was more likely to be barium oxalate. This sample thus probably consisted of barium carbonate, barium oxalate and unreacted bis(oxalato) cuprate(II). No estimate was made of the amount of each species present.

The DSC results confirmed that the decomposition occurred in several overlapping processes. The infrared spectrum of the solid intermediate at 320°C contained an absorption band due to the presence of the carbonate ion. The formation of barium carbonate (although perhaps in small quantities) thus occurs during the early stages of the decomposition.

A DSC curve for $Ba[Cu(C_2O_4)_2(H_2O)]\cdot 5H_2O$ heated at 20°C min^{-1} in N_2 is shown in Fig. 2, curve (a). The curve shows an initial endothermic process with an onset temperature of 75°C, and the maximum is reached at 160°C. At 250°C a second small endothermic peak occurs, but is soon swamped by an exothermic process with overall maximum at 305°C. A second exothermic maximum occurs at about 410°C. The DSC and DTG (Fig. 1) curves show some similarities.

The enthalpy for the dehydration, calculated from the area of the first peak, is 311±30 kJ mol^{-1}, or 52±5 kJ (mol of H_2O)$^{-1}$. The large uncertainty in this re-

sult arises from uncertainties in the baseline, since the dehydration continues until the onset of the decomposition. The second small endothermic peak (at 250°C), which precedes the large exothermic peak, indicates that the initial stages of the decomposition are endothermic.

The overall exothermic nature of the decomposition is of interest, since the decomposition of barium oxalate to barium carbonate (step (3)) is known to be endothermic. The exothermic peak must thus be largely due to step (2) above.

The decomposition of copper oxalate is strongly exothermic with onset at about 290°C [1] which supports the reaction proposed above, although the exotherm observed for pure copper oxalate is must narrower, and less intense (-33 kJ mol^{-1} compared to -347 kJ mol^{-1}) [1].

The thermal decomposition of pure BaC_2O_4 [6, 7] begins at 330°C and is complete at 550°C. The strong exothermic nature of reaction (1) would swamp any indication of the endothermic reaction. Also, the oxalate ion might be decomposing in a matrix different to that of pure barium oxalate. The TG results show that at 450°C the sample has reached its stable final mass corresponding to the formation of barium carbonate and copper metal. Since the thermal decomposition of $Ba[Cu(C_2O_4)_2]$ is complex with many overlapping processes (both exothermic and endothermic), accurate estimates of the enthalpy changes of the stages could not be made. An estimate of the overall enthalpy change was made by measuring the combined area of the overlapping peaks. This estimate of ΔH for the decomposition of $Ba[Cu(C_2O_4)_2]$ in N_2 is -347 kJ mol^{-1}.

The DSC curve for $Ba[Cu(C_2O_4)_2(H_2O)]\cdot 5H_2O$ heated in O_2 is shown in Fig. 2, curve (b). The complex nature of the decomposition is again apparent from this curve, which shows many similarities to the curve obtained in N_2 (curve (a)). As found in N_2, the initial endothermic process is soon swamped by the main exothermic process, but, in O_2, the maximum is reached sooner, and the main decomposition exotherm in O_2 is much narrower than in N_2. The several broad overlapping exothermic peaks may mask any endothermic processes.

Thermochemistry

The overall enthalpy change for the thermal decomposition of $Ba[Cu(C_2O_4)_2]$ in O_2 was estimated from the combined area of the overlapping peaks as -457 kJ mol^{-1}, compared with -347 kJ mol^{-1} estimated in N_2.

DSC runs in O_2 were used to estimate the enthalpy of formation of $Ba[Cu(C_2O_4)_2]$ because there are no uncertainties in the oxidation states of the products. The oxalate groups were completely oxidised to carbon dioxide and the copper was converted to copper(II) oxide. The overall reaction in O_2 is:

$$Ba[Cu(C_2O_4)_2](s) + O_2(g) \rightarrow BaCO_3(s) + CuO(s) + 3CO_2(g) \qquad (4)$$

which, again, can be divided into two steps:

$$Ba[Cu(C_2O_4)_2](s) + 0.5O_2(g) \rightarrow BaC_2O_4(s) + CuO(s) + 2CO_2(g) \quad (5)$$

$$BaC_2O_4(s) + 0.5O_2(g) \rightarrow BaCO_3(s) + CO_2(g) \quad (6)$$

A value for the enthalpy of formation of anhydrous barium oxalate was estimated, from the enthalpies of formation of $BaC_2O_4 \cdot 2H_2O$ and $BaC_2O_4 \cdot 1/2H_2O$: -1970 and -1522 kJ mol^{-1}, respectively, as about -1500 kJ mol^{-1}.

For step (6):

$$\Delta H(6) = \Delta_f H BaCO_3(s) + \Delta_f H CO_2(g) - \Delta_f H BaC_2O_4(s) = -113 \text{ kJ mol}^{-1}$$

The enthalpy change for the overall reaction (4) in O_2 was estimated from the DSC curve as -457 kJ mol^{-1}. The enthalpy of formation of $Ba[Cu(C_2O_4)_2]$ was thus estimated as:

$$\Delta_f H Ba[Cu(C_2O_4)_2](s) = -\Delta H(6) + \Delta_f H BaCO_3(s) + \Delta_f H CuO(s)$$

$$+ 3\Delta_f H CO_2(g) = -2099 \text{ kJ mol}^{-1}$$

A similar estimate in N_2 gave:

$$\Delta_f H Ba[Cu(C_2O_4)_2](s) = -\Delta H(1) + \Delta_f H BaCO_3(s) + \Delta_f H Cu(s)$$

$$+ \Delta_f H CO(g) + 2\Delta_f H CO_2(g) = -1771 \text{ kJ mol}^{-1}$$

The discrepancy between the two estimates is due to the uncertainties in the enthalpy values measured from the DSC curves and possible uncertainties in the oxidation states of the products in N_2.

The kinetics and mechanism of the isothermal dehydration of $Ba[Cu(C_2O_4)_2(H_2O)] \cdot 5H_2O$

Isothermal α-time curves

The kinetics and mechanism of the dehydration of $Ba[Cu(C_2O_4)_2(H_2O)] \cdot 5H_2O$ were determined using isothermal thermogravimetry in the temperature range 85 to 105°C, in an atmosphere of flowing N_2. The isothermal dehydration curves showed smooth, continuous, deceleratory mass losses suggesting that no stable intermediate hydrates are formed. The dehydration curves were deceleratory throughout with the final stages of the reaction being very slow, even at higher temperatures. At low temperatures, the final stages were too slow to enable the reaction to approach completion in a reasonable time. As the tempera-

ture was increased, the initial region became virtually linear. This behaviour is typical of reactions controlled by diffusion. At the lowest temperature used, 85°C, the sample lost 11.1% of its mass after 100 min, corresponding to loss of approximately three water molecules per formula unit. At the highest temperature used, 105°C, the extent of dehydration in 100 min had increased to 16.7%, corresponding to the loss of approximately five water molecules.

The curves of mass loss *vs.* time were converted to α-time curves, where α is the fractional dehydration calculated on the removal of five H_2O molecules, i.e. 18.6% of the original sample mass (Fig. 3).

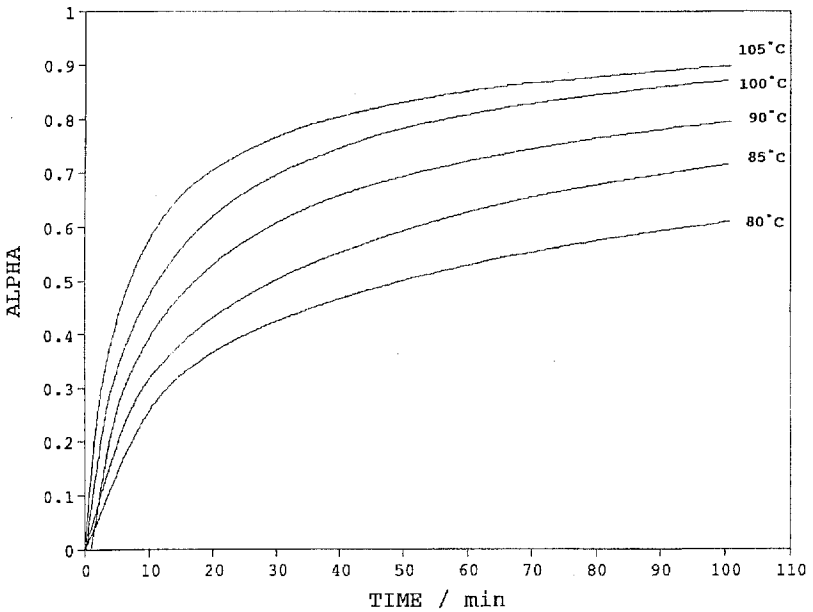

Fig. 3 Fraction of reaction (α) against time curves from isothermal TG experiments at 80, 85, 90, 100 and 105°C

The dehydration curve of crystals ground to a fine powder had a similar appearance to that of the original crystals, except that the initial stages were not as rapid and constituted a larger mass loss than the long, slow final stage of the dehydration.

Kinetic analysis

The most appropriate rate law which described the dehydration was determined by judging the linearity of the plots of the linear form of the standard deceleratory models ($g(\alpha)$) [8] against time. The diffusion models gave the best fits. Plots for the Jander equation (the three-dimensional diffusion (D3) model) were the most linear for all the isothermal dehydrations studied here. The good-

ness-of-fit, measured by the square of the correlation coefficient, r, for the linear regression and the associated rate constants for the different diffusion models, for the range $0<\alpha<0.77$, are shown in Table 1.

Table 1 The rate constants and goodness-of-fit (r^2) for the diffusion models at different temperatures for the isothermal dehydration of $Ba[Cu(C_2O_4)_2(H_2O)]\cdot 5H_2O$ (α range: 0.10 to 0.77)

Model	r^2	Rate constant, $k/10^{-3}$ min^{-1}
T=85°C		
D1	0.9606	3.54±0.03
D2	0.9755	2.37±0.02
D3	0.9997	0.73±0.04
D4	0.9980	0.56±0.04
T=90°C		
D1	0.9731	3.60±0.02
D2	0.9908	2.73±0.02
D3	0.9998	1.38±0.01
D4	0.9953	0.71±0.01
T=95°C		
D1	0.9769	5.34±0.01
D2	0.9799	4.03±0.05
D3	0.9999	2.57±0.01
D4	0.9965	2.05±0.06
T=100°C		
D1	0.9762	10.7±0.2
D2	0.9928	8.04±0.05
D3	0.9999	4.13±0.01
D4	0.9968	3.08±0.02
T=105°C		
D1	0.9601	30.3±0.3
D2	0.9972	22.5±0.2
D3	0.9962	6.78±0.01
D4	0.9882	5.54±0.03

The rate constants determined from the plots of the different diffusion models against time were used to calculate the theoretical curves of fractional dehydration (α) against time. A comparison of the calculated α-time curve, based on

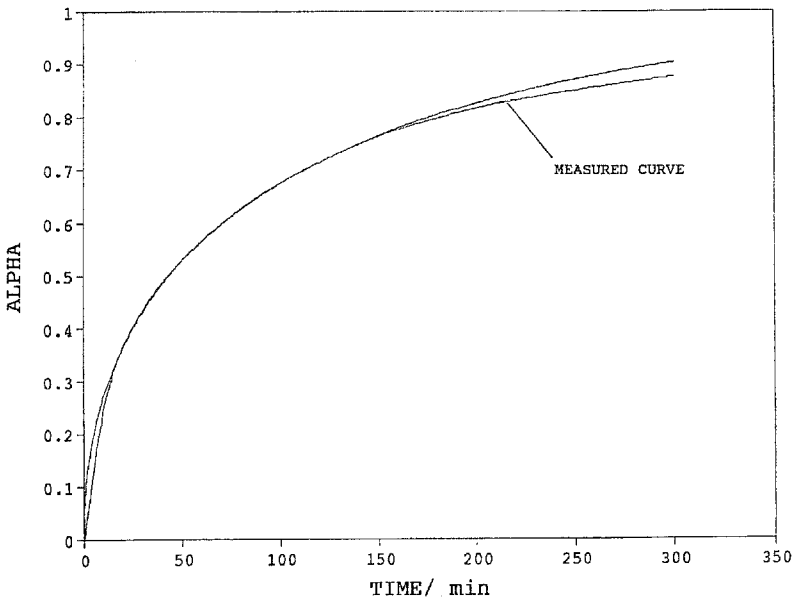

Fig. 4 Comparison between the calculated and the measured α-time curves for dehydration at 85°C

the Jander (D3) model, with the experimental $\alpha(t)$ curve at 85°C is shown in Fig. 4. Agreement is good over the range $0.20<\alpha<0.77$. The rate coefficients from the D3 model when used in an Arrhenius plot gave an apparent activation energy of 125±4 kJ mol^{-1} and pre-exponential factor of $(1.38\pm0.08)\times10^{15}$ min^{-1}.

The kinetics of the thermal decomposition of $Ba[Cu(C_2O_4)_2]$

Isothermal α-time curves

Isothermal TG experiments in N_2 at a series of temperatures between 230 and 260°C were used to determine the kinetics and the mechanism of the decomposition. Each sample was dehydrated under the same conditions before each run: heated to 180°C at a rate of 20°C min^{-1} and held at that temperature for 10 min, before increasing the temperature at 20°C min^{-1} to the value used to study the decomposition. The last traces of water were very difficult to remove and care had to be taken when deciding where the dehydration ended and where the decomposition began.

Although the temperature range of these isothermal runs is significantly lower than the temperatures reported at which the decomposition barium oxalate→barium carbonate takes place, IR spectroscopy of the solid residues showed that barium carbonate was present in the reaction product in significant proportions.

The mass-time curves are smooth and the different reaction steps do not show up in the isothermal decomposition. There is thus a problem in defining the extent of decomposition, α. At the highest isothermal temperatures used (260°C) (not shown), the mass tended towards a final value of 61%. Formation of barium oxalate and copper metal corresponds to a residue of 59.6% of the initial mass of the hydrate. The α-time curves were calculated on the basis of α=1.00 when the mass of the final solid residue is 59.6% of the initial mass of the hydrate. The α-time curves for the runs at 235, 240 and 250°C are shown in Fig. 5.

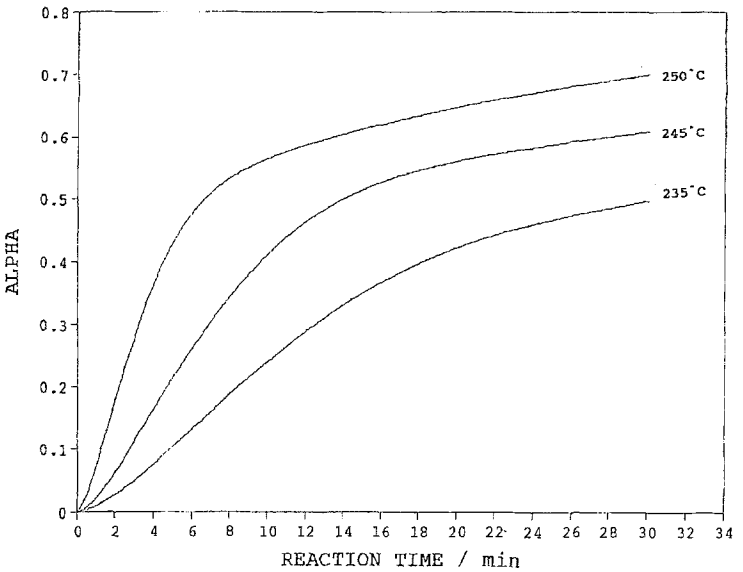

Fig. 5 Fraction of reaction (α) *vs.* time curves from isothermal TG experiments at 235, 240 and 250°C

The curves consist of at least three stages: (a) an initial acceleratory stage; (b) a deceleratory stage; and (c) a slow final stage. Stages (a) and (b) are far more rapid than the final stage. It is immediately qualitatively apparent that the initial stages (a) and, especially (b), have significant temperature dependences, whereas the final stage (c) has a lesser temperature dependence, remaining relatively slow over the whole temperature range and becoming negligibly slow, on the time scale used, at the low temperature end of the range (235°C). In attempting a kinetic analysis of the α-time curves given in Fig. 5, several simplifications were necessary. The initial acceleratory process which accounts for only a small portion of the decomposition was ignored. Its acceleratory nature is only clearly evident at the lower temperatures and, as the temperatures used were increased, this stage merges with the main stage (b). As an estimate of the kinetic parameters of stage (b), the slopes of the approximately linear regions of the α-time

curves were used as a measure of the rate coefficients. This is equivalent to assuming zero-order kinetic behaviour: $d\alpha/dt=k_o$. Since many deceleratory curves may be described by the 'order of reaction' type rate equations: $d\alpha/dt=k_n(1-\alpha)^n$, k_o is a good approximation for k_n, when α is small.

Values of k_o, when used in an Arrhenius plot (not shown), gave an activation energy, E_a, of 215±22 kJ mol^{-1} and pre-exponential factor, $A=(6.4\pm0.5)\times 10^{21}$ min^{-1}.

To make a more detailed kinetic analysis, it was necessary to attempt to separate the contribution of the final process (c) from that of (b). The decomposition was assumed to be described by a rate equation of the form: $d\alpha/dt=k_1f_1(\alpha)+k_2f_2(\alpha)$. The rate ($d\alpha/dt$) *vs.* time ($t$) curves were calculated using a 9-point Savitzky-Golay algorithm [9]. A typical plot of rate ($d\alpha/dt$) *vs.* time (for the experiment at 250°C) is shown in Fig. 6.

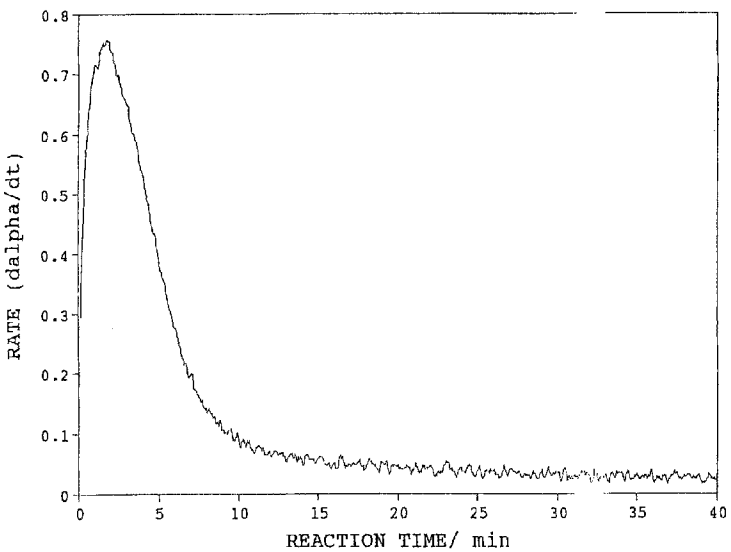

Fig. 6 Rate of reaction ($d\alpha/dt$) *vs.* time for the isothermal decomposition at 250°C

The later sections of the $d\alpha/dt$ curves are approximately linear. Such behaviour corresponds to the R2 model. The derivative form of the R2 model is: $d\alpha_2/dt=-2k_2(1-kt)=-2k_2+2k_2^2t$. Linear regression on the linear region was used to calculate k_2. The slow process, $k_2f(\alpha)_2$, was then substracted from the total rate to give rate$_1$. Rate$_1$ was then fitted empirically by an equation of the form: $d\alpha/dt=nk_1(1-k_1(t-t_o))^{(n-1)}$ which for the case of n=2, corresponds to the contracting-area equation (R2) and, for n=3, to the contracting-volume equation (R3) (t_o is a correction to the time scale to allow for the possibility that the model equation does not apply from the zero of the experimental curve). As the value of n is

increased, the concave-up shape of the resulting curve becomes more pronounced. k_1 was adjusted to bring the calculated curve into the required range.

Use of n=3 did not produce sufficient curvature, so it was decided to fit the experimental curves by empirical adjustment of the three variables n, k and t_o using a sum of squares of the residual deviations, Σ(rate(expt.)–rate(model))^2 to optimize the fit.

An alpha-time curve was then reconstructed from the two contributions: $d\alpha/dt = d\alpha_1/dt + d\alpha_2/dt$. By integration and suitable weighting,

$$\alpha_1 = \alpha(Rn) = 1 - (1 - k_1 (t - t_o))^{(n+1)}$$

$$\alpha_2 = \alpha(R2) = 1 - (1 - k_2 t)^2$$

$$\alpha_{TOTAL} = w_1\alpha_1 + w_2\alpha_2$$

Good matches were obtained by trial-and-error. The $d\alpha/dt$-time curve at 250°C is shown in Fig. 6. Linear regression over the time range 17 to 30 min gave a slope, $m_2 = -1.1\times10^{-4}$ and intercept, $c_2 = 2k_2 = 1.5\times10^{-2}$. The rate constant, k_2 was estimated from the slope of the regression ($k_2 = 7.4\times10^{-3}$ min^{-1}). This value for k_2 was used to calculate, and hence subtract, rate$_2$ from the overall rate to give rate$_1$. The corrected plot of rate$_1$ *vs.* time is shown in Fig. 7. The optimized fit occurred when n=5, k_1=0.056 min^{-1}, and t_o=–1.45 min and this is also shown in

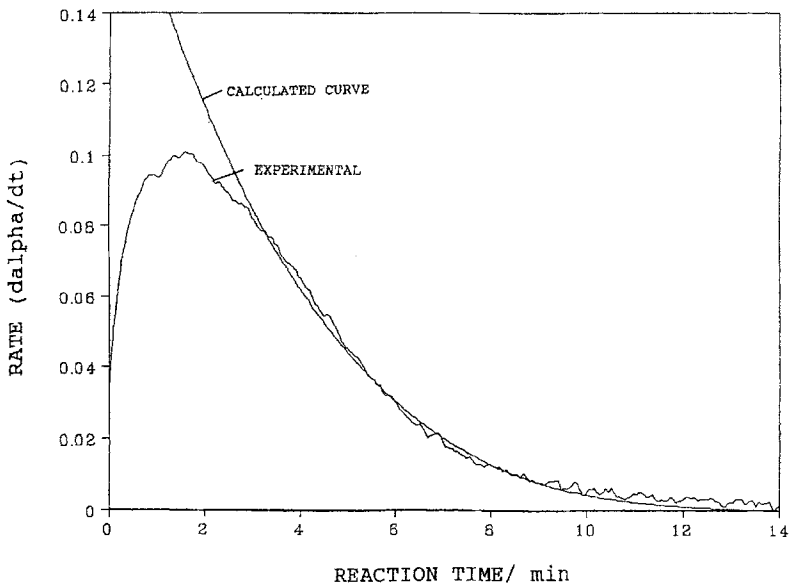

Fig. 7 Corrected rate of reaction ($d\alpha_1/dt$) *vs.* time curve for the decomposition at 250°C, compared with the calculated $d\alpha_1/dt$ curve: k_1=0.056 min^{-1}, n=5, and t_o=–1.45 min

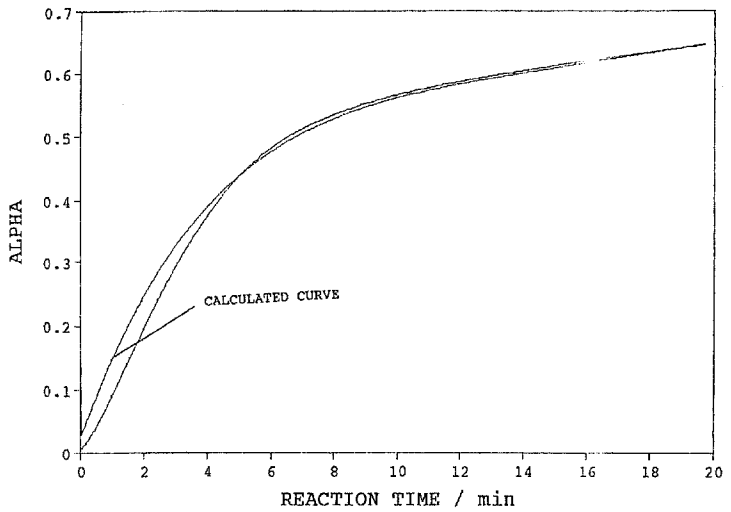

Fig. 8 Comparison between the calculated and experimental α-time curves for decomposition at 250°C

Fig. 7. The α-time curve was then reconstructed from the two contributions, $rate_1$ and $rate_2$. A good match between the experimental and calculated α-time curves was obtained with the following: w_1=0.48, k_1=0.056 min^{-1}, t_o=0 min, n=5, and w_2=0.62, k_2=0.073. This is shown in Fig. 8.

The values of the kinetic constants obtained in the series of isothermal experiments are summarized in Table 2.

Table 2 Kinetic parameters for the thermal decomposition

T/°C	n	t_o/min	k_1/min^{-1}	$k_2/10^{-3}$ min^{-1}	w_1	w_2
235	5	−5	0.015	1.2	0.5	0.6
240	5	2.0	0.029	3.0	0.5	0.6
250	5	−1.5	0.056	7.4	0.5	0.6
255	5	0	0.078	8.7	0.5	0.6
260	5	−0.48	0.19	32.2	0.5	0.5

The rate constants for the fast process (k_1) and the slow process (k_2) were used in Arrhenius plots and values of E_a and A of 206±23 kJ mol^{-1} and $(2.2\pm0.5)\times10^{19}$ min^{-1}, for the fast process, and 259±37 kJ mol^{-1} and $(6.3\pm1.8)\times10^{23}$ min^{-1} for the slow process, respectively, were obtained.

Discussion

Dehydration

The results of the kinetic analysis, suggest that the rate determining step in the dehydration of $Ba[Cu(C_2O_4)_2(H_2O)]\cdot 5H_2O$ is the three-dimensional diffusion of water vapour through the layer of solid product. X-ray diffraction results [4] have shown that $Ba[Cu(C_2O_4)_2(H_2O)]\cdot 5H_2O$ contains water molecules in different environments. One water molecule is directly bonded to the copper(II) ion, the five remaining water molecules are weakly held to the barium ion. The barium-water distances vary. The water molecules which are not complexed to the copper(II) take part in hydrogen bonding to each other and to the dioxalato-anion. The rate limiting step in the overall process of dehydration is the diffusion of the product gases through the layer of solid product, so differences in the way the water molecules are held in the crystal will not show up in the isothermal dehydration. This could be visualised in terms of a build up of water, already dissociated from its original sites, in pockets or chambers in the crystal, waiting to escape.

The apparent activation energy for the dehydration (125 ± 4 kJ mol^{-1}) of $Ba[Cu(C_2O_4)_2(H_2O)]\cdot 5H_2O$ is significantly less than the enthalpy of reaction (ΔH=311±30 kJ (mol of complex)$^{-1}$). According to the transition state reaction profile of an endothermic reaction, the activation energy, E_a, for an endothermic process cannot be less than the enthalpy of reaction, ΔH. The problem, however, lies in reconciling the definitions of the amount of substance referred to in the E_a and ΔH values. The mole upon which the E_a value is based arises through the use of the gas constant, R and hence, in terms of transition state theory, would refer to 'mole of activated complexes'. Enthalpy values, however, are based upon a stated stoichiometry which can be adjusted as required. On the presumption that $E_a \geq \Delta H$ when the mole referred to is the same amount of material, it may be necessary to divide ΔH by a factor n. In this case $\Delta H/6$ is equal to 51.8 kJ mol^{-1}. This value may be compared with the enthalpy of vaporisation of water (40.7 kJ mol^{-1}). The isothermal dehydration of copper(II) sulphate pentahydrate has been described as being analogous to the evaporation of water [10]. However, as mentioned above, the rate determining step is not the process of breaking the bonds which hold the water molecules (hydrogen bonds etc.) in the crystal lattice, but the transport of the dissociated water molecules through the solid. Therefore, on this basis alone, the complete process of the isothermal dehydration of $Ba[Cu(C_2O_4)_2(H_2O)]\cdot 5H_2O$ is not analogous to the evaporation (although certain steps in the overall process may be similar). The activation energy for the isothermal dehydration of $K_2[Cu(C_2O_4)]\cdot 2H_2O$ was reported to be 116 kJ mol^{-1} [11]. Insausti *et al.* [12] prepared $Sr_2[Cu(C_2O_4)_3(H_2O)_2]\cdot 5H_2O$ as a possible precursor to the mixed oxide Sr_2CuO_3. TG studies showed that dehydration oc-

curred in three consecutive endothermic steps (2:2:3). The ΔH for the overall dehydration was 54 kJ mol^{-1}.

Decomposition

The slow process can be described in terms of the conventional contracting-area model (R2). Applicability of such a model is compatible with the kinetics of the dehydration process and could indicate progress of the reactant/product interface for this decomposition process along similar paths to those followed during removal of water from the hydrate. The prior removal of water would create pores or pathways which could be used, at higher temperatures, for the relatively unhindered removal of decomposition products.

The more rapid concurrent process, after the contribution from the slow process had been subtracted, was not readily describable by the conventional set of kinetic models [8].

The empirical model used to describe the faster process:

$$d\alpha/dt = nk_1 (1 - k_1 (t - t_o))^{(n-1)}$$

with n=5 and very small values of t_o corresponds then to an α, time relationship of the form

$$\alpha = 1 - (1 - kt)^5$$

The α, time curve for this R5 model is slightly more sharply deceleratory than the R3 curve, but is not as deceleratory as the diffusion models, e.g., D3. No reference to the use of a value of n>3 for the contracting-geometry model (Rn) was found, but a possible justification for such a value may arise for a system where diffusion and geometric factors are fairly evenly balanced and neither is totally dominant.

Conclusions

The X-ray structure analysis of $Ba[Cu(C_2O_4)_2(H_2O)]\cdot 5H_2O$ [4] showed that the crystal consists of linear chains of monomeric units of aquodioxalato copper(II) weakly bridged by barium ions. The barium ions are surrounded by 11 oxygen atoms. Two of these atoms (O(10) and O(12)) were closer than the sum of the covalent radius of O^{2-} and ionic radius of Ba^{2+}. The coordination geometry of the copper(II) ion could be considered to be square pyramidal with some trigonal distortion. The equatorial positions were occupied by the oxalate ions, and the axial position by a water molecule.

The dehydration of $Ba[Cu(C_2O_4)_2(H_2O)]\cdot 5H_2O$ took place at lower temperatures (~90°C) than the monooxalates (typically>140°C). This is because most of

the water which is lost is weakly bound to the barium ions, whereas in the monooxalates the water is directly coordinated to the metal ions. During the dehydration, the number of water molecules stabilising the positive charge of the barium ion is decreased. Insausti *et al.* [12] suggest that the dehydration is probably accompanied by the rearrangement of the ligands (oxalate ions and remaining water molecules) about the metal centres.

The kinetics of the isothermal dehydration of $Ba[Cu(C_2O_4)_2(H_2O)]\cdot 5H_2O$ were strongly deceleratory and could be described by the three-dimensional diffusion (D3) model. The different environments of the water molecules did not appear to influence the kinetics of the isothermal dehydration. The activation energy measured was 125 ± 4 kJ mol^{-1} and the preexponential factor was $1.38\pm0.08\times10^{15}$ min^{-1}. The onset of the decomposition coincided with the loss of the final traces of water.

There is some evidence to suggest that the rate-limiting step in the decomposition of copper oxalate is electron transfer from the oxalate ions to the copper ions [13]. In $Ba[Cu(C_2O_4)_2(H_2O)]\cdot 5H_2O$, electron transfer can conceivably take place from the oxalate ions to the copper(II) ions or the barium ions. The barium ion is a very poor electron acceptor compared to the copper(II) ion so electron transfer to the copper(II) ion is more probable. One of the two oxalate groups is positioned more closely to the barium ion and it is thus likely to be more stable with respect to electron transfer. The C–C bond of the oxalate group which is further away from the barium ion may thus break and release carbon dioxide, while the second oxalate group, positioned more closely to the barium ion, remains intact. At higher temperatures, the second oxalate ion decomposes but, since the barium ion is such a poor electron acceptor, the oxalate decomposition is associated with the formation of barium carbonate.

The kinetics of the decomposition of copper(II) oxalate are complex, with no single rate law adequately describing the entire decomposition [13]. The kinetics of the decompositions of the mixed metal oxalates ($MCu(ox)_2\cdot 3H_2O$) [2] were also complex and the isothermal rate-time curves could be described in terms of several concurrent sigmoid and deceleratory processes. The isothermal rate-time curves for the decomposition $Ba[Cu(C_2O_4)_2(H_2O)]\cdot 5H_2O$ consisted of concurrent processes, which were separated into a slow process and a fast process. The fast process could not be described by the conventional geometrical models, but the contracting-geometry model, with n=5, gave a good description. The slow process could be described by the conventional contracting-area (R2) model. The α-time curves of all the mixed metal oxalates showed an initial fast process and a second, slower process ($0.5<\alpha<0.8$). The slow process (an overlap of two sigmoidal processes) was deceleratory and could be described by the contracting-volume (R3) equation. Since the later stages of the decomposition of the mixed metal oxalates ($MCu(C_2O_4)_2$), and $Ba[Cu(C_2O_4)_2]$ could be described by the contracting-geometry (Rn) equation, the Arrhenius parameters for the later

stages of all the decompositions are comparable. Arrhenius plots for the second stage of the decompositions of the mixed metal oxalates, $MCu(C_2O_4)_2$, gave activation energies of 155±40, 101±16 and 91±2 kJ mol^{-1} for M=Fe, Co and Ni. An Arrhenius plot for the second, deceleratory process of the decomposition of $Ba[Cu(C_2O_4)_2]$ gave an activation energy of 259±37 kJ mol^{-1}.

It is suggested that removal of the bulkier gaseous products of the decomposition (CO_2 and CO) occurs through channels made by the prior dehydration, and that the kinetic behaviour is on the borderline between control by geometrical progression of the reactant/product interface and control by diffusion.

References

1 A. Coetzee, D. J. Eve and M. E. Brown, J. Thermal Anal., 39 (1993) 947.
2 A. Coetzee, D. J. Eve, M. E. Brown and C. A. Strydom, J. Therm. Anal., 41 (1994) 357.
3 A. Bouayad, J.-C. Trombe and A. Gleizes, Inorg. Chim. Acta, 230 (1995) 1.
4 J. Bacsa, M. Sc. Thesis, Rhodes University, 1995.
5 M. Isausti, R. Cortes, M. I. Arriortua, T. Rojo and E. H. Bocanegra, Solid State Ionics, 63–65 (1993) 351.
6 A. H. Verdonk and A. Broersma, Thermochim. Acta, 6 (1973) 95.
7 N. Koga and H. Tanaka, J. Thermal Anal., 32 (1987) 1521.
8 M. E. Brown, D. Dollimore and A. K. Galwey, 'Reactions in the Solid State', Comprehensive Chemical Kinetics, Vol. 22, Elsevier, Amsterdam 1980.
9 A. Savitsky and M. J. E. Golay, Anal. Chem., 8 (1964) 680.
10 W.-L. Ng, C.-C. Ho and S.-W. Ng, J. Inorg. Nucl. Chem., 34 (1978) 459.
11 J. E. House and L. A. Marquadt, J. Solid State Chem., 89 (1990) 155.
12 M. Isausti, M. K Urtiaga, R. Cortes, J. L. Mesa, M. I. Arriortua and T. Rojo, J. Mater. Chem., 4 (1994) 1867.
13 M. A. Mohamed and A. K. Galwey, Thermochim. Acta, 213 (1993) 269.